

JOURNAL OF MECHANICS OF CONTINUA AND MATHEMATICAL SCIENCES

www.journalimcms.org



ISSN (Online): 2454 -7190 Vol.-20, No.-11, November (2025) pp 1-19 ISSN (Print) 0973-8975

DYNAMIC AND STRUCTURAL OPTIMIZATION OF THE TOWERS'S CENTRAL CORES BRACING FOR TARGETED DESIGN AND UPGRADED SEISMIC RESPONSE

T. El Bahlouli¹, O. Hniad²

¹ Earth Sciences Department, Higher National School of Mines Rabat (ENSMR), Agdal-Rabat, Morocco-753.

²Civil Engineering Department, Mohammadia Engineering School (EMI), Agdal-Rabat, Morocco-765.

Email: 1elbahlouli@enim.ac.ma, 2hniad@emi.ac.ma

Corresponding Author: Tarik El Bahlouli

https://doi.org/10.26782/jmcms.2025.11.00001

(Received: July 29, 2025; Revised: October 12, 2025; October 30, 2025)

Abstract

This study introduces a parametric preliminary design of central core bracing tailored for towers and tall buildings dominated by dynamic flexural vibrations and handled by accidental and serviceability deflections. In such slender systems, the determination of the core thickness is of critical importance to structural engineers, as it formally validates the pre-project stage and, subsequently, enables proper structural detailing outcomes in accordance with seismic regulations and technical standards. This issue is a real challenge, as it typically entails an unlimited number of attempted iterations and enormous computational time to converge towards the optimal values of the structural load-bearing elements.

To address this problem, we introduce a streamlined methodological approach, structured as a practical guideline, aimed at defining an optimal variation of the thickness profile and facilitating accurate structural sizing. This dynamic and structural optimization is governed by the max-min formulation of the natural frequency eigenvalue. For this, two strategic zones, depending on the height of the tower, were delineated. Additionally, the construction material usage quantity constraint is imposed to ensure its optimal consumption, thereby establishing a bridge between structural design maturity and the ambitions for increasing profits and resource savings. The principal advantage of this mechanical and mathematical resolution lies in its simplicity and practicality, allowing rapid and efficient hand-use calculations.

The present paper is crowned by an illustrative case study designed to evaluate the tangible benefits achieved through the dynamic modal analysis.

Keywords: Central Core Bracing, Dynamic Behavior, Material Optimization, Natural Frequency, Seismic Response, Tower, Tall-Building, Thickness Variation.

I. Introduction

Our new era is increasingly defined by a prominent and visible urbanization pressure. Consequently, the development and planning of strategic land-use zoning specifically dedicated to high-rise buildings and tall towers have become a real imperative and a critical necessity, aiming to accommodate the escalating demand among urban populations for spatially efficient and functionally optimized residential and office spaces. This can be considered a fundamental phenomenon in the current urbanization [I].

This further underscores the fact that tall buildings and tower developments offer a genuine opportunity for real estate investors and developers seeking not only to maximize the profitability per square meter of land but also to accelerate the return on investment timelines [XIV].

From a strictly mechanical and structural standpoint, the projected floor's number induces a significant seismic effect on such tall structures [VI], and it becomes a priority to safeguard human lives and mitigate structural damage by developing effective solutions to ensure safety under various loading conditions and improve overall stability [II]. Therefore, their structural design cannot be limited to a mere transcription of architectural conceptual drawings and plans.

Indeed, numerous studies [V] [XIII] [XVII] concur on the inherent complexity of structural dynamic analysis, emphasizing that the height of slender towers constrains civil engineers within highly sensitive computational outputs. This sensitivity stems from the strong interdependence with input parameters and data, particularly the dimensions of structural load-bearing elements and the bracing system's positioning.

In this context, the dynamic response of high-rise buildings and tall towers results from a refined and targeted balance between several fundamental parameters [IX] [XVI] [XVII], such as the horizontal and vertical stiffness or inertia distribution, mass distribution in-plane and along the height, the geometric and dimensional characteristics of bracing structural elements, and their specific configuration.

In the same frame, besides global dynamic properties, the resilience (ultimate strength–deformation capacity) of a shear-wall-braced structure also depends on its symmetry, which enhances the perceived regularity and upgrades its seismic response, as demonstrated by Patil et al. [XV]. This rationale underpins our decision to orient this research paper toward central-core bracing systems.

Translating these principles into a reliable numerical model requires a realistic and accurate dynamic behavior representation. In this regard, the in-depth work of Dym and Williams [VII] has highlighted the limitations of simplified classical models, which are often unable to accurately predict the vibratory behavior of tall buildings.

Furthermore, as emphasized by Paz and Leigh [XVI], a uniform stiffness distribution along the entire height of a building tends to concentrate seismic forces at the base,

which amplifies differential displacements and exacerbates structural vulnerability. In contrast, a degressive distribution - i.e., a stiffness or flexural inertia that decreases with altitude significantly enhances and upgrades the Structural Accidental State response, reduces base-level stresses in Ultimate Limit State, and improves the mastery of Serviceability-Limit State deflections.

This approach is further supported by the insightful parametric study of Alavi et al. [III], whose model integrates a minimum stiffness constraint for optimizing lateral stability. They advocate for abandoning homogeneous stiffness or constant inertia assumptions in favor of variable parametric distributions, which are better suited to current trends and modernist dynamic modeling requirements.

In its turn, too, the work of Rahgozar et al. [XVIII] proposed an analytical formulation based on Timoshenko beams with variable cross-sections, allowing for the adjustment of natural frequencies and vibration modes in slender structures.

This overall trend is likewise supported by Nieto et al. [XII], who concur on the necessity of designing an optimized thickness profile to reconcile structural efficiency with profitability and, consequently, with cost rationalization. The study carried out by Lam and Ho [X] corroborates this conclusion. It provides concrete evidence of the influence of shear-wall thickness on dynamic structural behavior and how it affects the internal forces and horizontal displacements.

A range of approaches is still evolving toward material optimization and efficiency, involving increasingly high degrees of complexity that require advanced analytical methodologies. One of these is the novel hybrid optimization framework for sizing shear wall high-rise buildings proposed by Haopeng et al. [VIII], which combines the discrete particle swarm optimization (PSO) technique with the response surface method.

This paper is intended to develop a simple, practical, and functional guideline for the parametric pre-sizing of slender towers by central core bracing (with shear walls). This guideline is intended for use during preliminary structural designs and assessments, a critical milestone for iterative engineering convergence between dynamic structural design and seismic performance improvement.

Accordingly, this study relies on the free vibration equation of a cantilever beam (fixed at its base and free at its top) [XVI], and incorporates mechanically intuitive parameters easily grasped by practicing civil engineers, such as wall thickness, inertia, natural frequency, fundamental pulsation, and general/interstory displacement. This easy-to-use parametric study fully aligns with the goals of financial optimization, resource rationalization, and effective upgrading of both modal dynamic response and seismic performance, through the targeted adjustment of the fundamental frequency of the modeled structural system.

II. Mechanical Formulation of Dynamic Structural Behavior with Distributed Properties

The dynamic analysis of structures, represented through lumped parameter models with discrete coordinates for single-degree-of-freedom systems and for multi-

degree-of-freedom systems [XX], offers a good methodology for evaluating structural behaviors under dynamic loads. Nonetheless, this modeling yields only rough results of the real dynamic response. This is added to the fact that these structures possess continuous distributed properties with an unlimited degrees of freedom [XVI].

The present paper is based on the dynamic theory of beams. For this reason, the treatment of our towers and tall buildings is based on the simple bending theory of a cantilever beam (one end fixed and the other end free), as it is commonly used for engineering purposes [XVI]. This beam model is thus assumed to exhibit distributed mass and elasticity. This is shown in Figure 1.

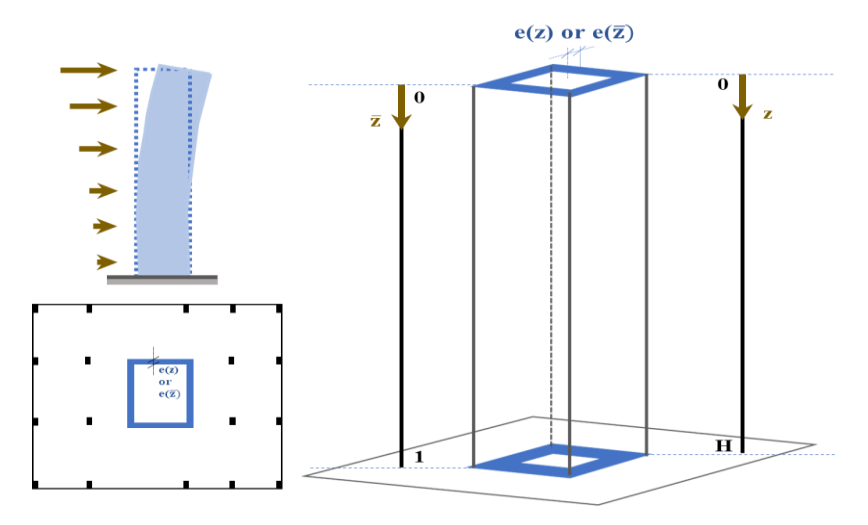


Fig. 1. Plan view of a typical floor, elevation view of the shear wall, and a 3D perspective of the central core bracing system.

The origin of the vertical coordinate axis z is defined at the free end, positioned at the top of the tower. The positive z-axis extends downward. The base, representing the fixed end, is positioned at z = H, where H corresponds to the total height of the tower.

Accordingly, and for the purposes of streamlining and broadening the applicability of the proposed solution, we shall adopt the following formulation:

$$\bar{z} = Z/H \tag{1}$$

The plane's lateral displacement in the perpendicular direction of the z (or \overline{z}) axis is denoted by y. It can be expressed as the product of two separate functions: a function of deflection position $\Delta(z)$ (or $\Delta(\overline{z})$) and a function of time $\varepsilon(t)$ [XVI], that is:

$$y(z,t) = \Delta(z) \cdot \varepsilon(t) \tag{2}$$

Hence, based on Figure 1, the boundary conditions for this cantilever beam, considering overdots indicate derivatives with respect to z, are as follows:

• At the free end (top of the tower): That is, at $z = \overline{z} = 0$, the bending moment M and the shear force V must be zero:

Condition 1:
$$\Delta(z=0) = \Delta_{max} \rightarrow \dot{\Delta}(z=\bar{z}=0) = 0$$
 (3)

Condition 2:
$$M(0,t) = 0 \to \ddot{y}(0,t) = 0 \to \ddot{\Delta}(z = \bar{z} = 0) = 0$$
 (4)

Condition 3:
$$V(0,t) = 0 \rightarrow \dot{y}(0,t) = 0 \rightarrow \dot{Z}(z = \bar{z} = 0) = 0$$
 (5)

• At the fixed end (recessed end of the tower): that is, at z = H or, $\bar{z} = 1$, the deflection and the slope must be zero:

Condition 4:
$$y(H,t) = 0 \rightarrow \Delta(z = H) = \Delta(\bar{z} = 1) = 0$$
 (6)

Condition 5:
$$\dot{y}(H,t) = 0 \rightarrow \dot{\Delta}(z=H) = \dot{\Delta}(\bar{z}=1) = 0$$
 (7)

While solving such equations analytically is generally more complex than discrete methods, the study of continuous systems, particularly for simple structural configurations, yields valuable insights and outcomes with relatively modest computational effort. As a matter of fact, such analyses play a crucial role in assessing approximate methods based on discrete models. Acceleration, as well as variations in shear force and bending moment, are described using partial derivatives since these quantities depend simultaneously on two variables: the spatial coordinate **z** along the tower (modeled by a beam) and the temporal variable t [XVI].

Assuming that shear deformation, rotary inertia, and damping are neglected, the lateral flexural equation of free vibration of a cantilever beam according to the perpendicular motion to the z [XVI], is:

$$EI(z) \cdot \frac{\partial^4 y}{\partial z^4} + m \cdot \frac{\partial^2 y}{\partial t^2} = 0$$
 (8)

Where E is Young's modulus of elasticity,

And I(z) represents the moment of inertia associated with the transverse section of the hollow central core. It is defined by :

$$I(z) = I_0 \cdot e(z) \tag{9}$$

Considering that e(z) denotes the core thickness as a function of the vertical coordinate, as shown in Figure 1.

And I₀ corresponds to the moment of inertia of the core with a unit thickness.

The substitution of equations (2) and (9) in the differential equation (8) leads to :

$$\frac{\partial^2 \varepsilon(t)}{\partial t^2} + \left[\frac{EI_0}{m} \cdot \frac{\frac{\partial^2}{\partial z^2} (e(z) \cdot \ddot{\Delta}(z))}{\Delta(z)} \right] \cdot \varepsilon(t) = 0$$
 (10)

$$\operatorname{Or}: \frac{\partial^{2} \varepsilon(t)}{\partial t^{2}} + \left[\sqrt{\frac{EI_{0}}{m}} \cdot \Omega \right]^{2} \cdot \varepsilon(t) = 0$$
 (11)

Where :
$$\Omega^2 = \frac{\frac{\partial^2}{\partial z^2} (e(z).\ddot{\Delta}(z))}{\Delta(z)}$$
 (12)

Considering that ω represents the angular frequency of the beam. This natural frequency of the system is written as follows:

$$\omega^2 = \frac{EI_0}{m} \cdot \Omega^2 \tag{13}$$

A clear proportionality and dependence can be readily inferred between Ω and the natural frequency.

Then,
$$\frac{\partial^2}{\partial z^2} \left(e(z) . \ddot{\Delta}(z) \right) - \Omega^2 . \Delta(z) = 0$$
 (14)

III. Formulation of the Optimization Problem

In this section, we shall begin by refining the scope of our research problem, which will subsequently enable us to formulate it mathematically as a max-min model, subject to a set of technical constraints.

Mathematical and technical basis and framing of the problem

By adhering closely to the analytical implications of equation (13) and given that e(z) is the sole unknown for us, the problem is essentially linked with the optimization of the fundamental natural frequency. For this dynamic design optimization, it is standard practice to maximize the eigenvalue of the fundamental natural frequency to avoid the risk of resonance [XXII]. The latter, of course, is associated with its smallest value [IV] [XXI], denoted here ω_f . Considering the variable component of equation (13), and for the sake of convenience, our focus shall, by transitivity, be directed solely toward the variable Omega Ω . Consequently, Ω_f is utilized as the objective function within our proposed optimization model, which is expressed through a max-min formulation.

This governing parameter plays a critical role in regulating the dynamic response of the structure, in accordance with optimal determination of the vertical variation of the central core's thickness e(z). This approach effectively contributes to reducing the quantity and consumption of construction materials, such as reinforced concrete, for instance, and consequently results in a cost-effective solution driven by a targeted design strategy and upgraded seismic response.

To faithfully adhere to this underlying rational design framework, an initial constraint is imposed on the thickness function by stipulating that the iterative parameter, used for targeted optimization - aimed at reducing material consumption -, is the average thickness of the entire structure, denoted by e_m . A second constraint is defined by the parameter e_{min} , representing the minimum core thickness as mandated by current seismic design regulations and standards. This minimum thickness is applied to the upper stories of the tower, where the bending moment effectively is zero at the top (M=0). For the lower stories, the thickness varies but consistently remains strictly greater than the prescribed positive minimum throughout the entire structural height.

This formulation highlights the existence of a critical point, denoted $z_{cr} \in [0, H]$ or $\bar{z}_{cr} \in [0, 1]$, which delineates the structure into two distinct zones as shown in Figure 2: Constant Thickness Zone (CT) and Variable Thickness Zone (VT):

■ For CT Zone:
$$\forall z \in [0, z_{cr}]$$
: $e(z) = e_{CT}(z) = e_{min}$
or, $\forall \bar{z} \in [0, \bar{z}_{cr}]$: $e(\bar{z}) = e_{CT}(\bar{z}) = e_{min}$ (15)

• For VT Zone: $\forall z \in [z_{cr}, H]: e(z) = e_{VT}(z)$

or,
$$\forall \bar{z} \in [\bar{z}_{cr}, 1] : e(\bar{z}) = e_{VT}(\bar{z})$$
 (16)

In the CT Zone, the core thickness remains constant, resulting in a constant flexural rigidity EI. Consequently, the modal deformation is directly proportional to the bending moment, which varies along the vertical axis, and therefore, the curvature within this zone is necessarily non-uniform.

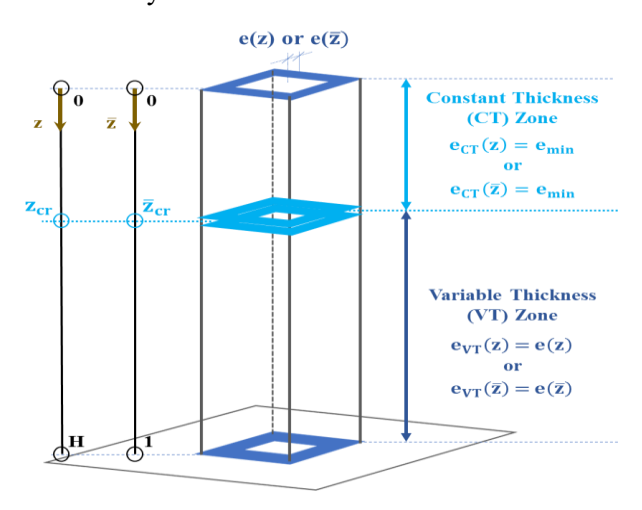


Fig. 2. Tall Tower divided into two zones according to central core thickness.

In contrast, the VT Zone allows for a gradual adjustment of thickness, and thus of rigidity. As previously suggested, it is possible to adopt a thickness variation law such that changes in bending moment are counterbalanced by corresponding changes in flexural rigidity governing which depends on the eigenvalue of natural frequency [IV] [XXI].

This approach may yield a more regular and controlled modal deformation in the lower part of the structure, harmonized with the frequency optimization governed by the max—min formulation. The curvature in this zone is therefore constant.

Mathematical and technical formulation of the problem

Based on the framework established with respect to the desired dynamic behavior of the tower's central core bracing, the problem addressed in the present paper can be formulated as follows:

$$\begin{cases} Max\{\Omega_f^2 = Min(\Omega_i^2)\}; i = 1, 2, \dots, +\infty \\ Subject to: \begin{cases} \int_0^H e(z)dz = e_m.H \\ \forall z \in [0; H]: 0 < e_{min} \le e(z) \end{cases} \end{cases}$$

$$(17)$$

Or,
$$\begin{cases} Max\{\Omega_f^2 = Min(\Omega_i^2)\}; i = 1, 2, \dots, +\infty \\ Subject to: \begin{cases} \int_0^1 e(\bar{z})d\bar{z} = e_m \\ \forall \, \bar{z} \in [0; 1]: 0 < e_{min} \le e(\bar{z}) \end{cases} \end{cases}$$
(18)

Consequently, two additional boundary conditions can be inferred as a direct outcome of incorporating the aforementioned critical point :

• Displacement continuity condition:

Condition 6:
$$\Delta_{CT}(z_{cr}) = \Delta_{VT}(z_{cr})$$
, or $\Delta_{CT}(\bar{z}_{cr}) = \Delta_{VT}(\bar{z}_{cr})$ (19)

• Slope continuity condition:

Condition 7:
$$\dot{\Delta}_{\text{CT}}(z_{\text{cr}}) = \dot{\Delta}_{\text{VT}}(z_{\text{cr}}), \text{ or } \dot{\Delta}_{\text{CT}}(\bar{z}_{cr}) = \dot{\Delta}_{\text{VT}}(\bar{z}_{cr})$$
 (20)

IV. Solution of the Optimization Problem

The resolution of our optimization system is structured around five key steps, as detailed below:

Key Step 1: Rayleigh-Ritz energy method

By using the Rayleigh-Ritz energy method, we can consider the Rayleigh quotient to be approximately equal to the system's natural frequency. This is deduced from the conservation of energy, where the equality between the average kinetic and potential energies is considered.

Based on equations (11) and (13):
$$R(\omega) = \omega^2$$
 (21)

This implies considering the orthonormality of the eigen-vectors and the equation (13), that:

$$\omega_n^2 = \frac{\int_0^H EI_0.e(z).[\ddot{\Delta}(z)]^2 dz}{\int_0^H m.[\Delta(z)]^2 dz} = EI_0. \int_0^H e(z). [\ddot{\Delta}(z)]^2 dz = \frac{EI_0}{m}. \Omega_f^2$$
 (22)

Then:
$$\Omega_f^2 = m \cdot \int_0^H e(z) \cdot [\ddot{\Delta}(z)]^2 dz$$
 (23)

Key Step 2: Lagrange multipliers method

To find the local maxima and minima of the objective function in equation (17) subject to equality constraints, we use the method of Lagrange multipliers. The corresponding Lagrangian is formulated, taking into account equation (23), as follows:

$$\mathcal{L} = \Omega_f^2 - \lambda \cdot \left(\int_0^H e(z) \cdot dz - e_m \cdot H \right)$$
 (24)

Where: $\lambda \ge 0$ denotes the Lagrange multiplier.

Or,
$$\mathcal{L} = m \cdot \int_0^H \left[\ddot{\Delta}(z) \right]^2 \cdot e(z) \cdot dz - \lambda \cdot \int_0^H e(z) \cdot dz + \lambda \cdot e_m \cdot H$$
 (25)

Among the critical points of the Lagrangian is the condition that its derivative with respect to e must be zero. Then, $\frac{\delta \mathcal{L}}{\delta e} = 0$ (26)

Which means that:

$$\frac{\delta \mathcal{L}}{\delta e} = \int_0^H (m. \ddot{\Delta}_f^2 - \lambda) \cdot \delta e \cdot dz = 0$$
 (27)

So, given that the curvature $\ddot{\Delta}_{VT}$ in the VT Zone (Variable Thickness) is constant – a meticulously validated corollary -, it follows that:

$$\ddot{\Delta}_f(z) = \ddot{\Delta}_f = \pm \sqrt{\lambda/m} = \pm \nu = Constant \, Value = \ddot{\Delta}_{VT}$$
 (28)

Key Step 3: The deflection position function

The deflection position function $\Delta(z)$ (or $\Delta(\bar{z})$), represents the modal displacement shape and is defined separately over the two structural regions as follows:

VT Zone :

By leveraging the preceding equation (28) and performing a double integration while applying the associated boundary conditions (conditions 5 and 4) specified, respectively, in equations (7) then (6), the following expression is obtained:

$$\Delta_{VT}(z) = \frac{1}{2}\nu.(z - H)^2$$
 (29)

Alternatively, the formulation can be expressed using the relative height variable defined in equation (1): $\Delta_{VT}(\bar{z}) = \frac{1}{2}\nu.H^2.(\bar{z}-1)^2$ (30)

For the sake of simplification, the following formulation may be considered:

$$\forall \, \bar{z} \in [\bar{z}_{cr}; 1]: \Delta_{VT}(\bar{z}) = \psi_{\nu}. \bar{\Delta}_{VT}(\bar{z}) \tag{31}$$

By defining new variables:
$$\psi_{\nu} = \frac{1}{2}\nu H^2$$
 and $\bar{\Delta}_{VT}(\bar{z}) = (\bar{z} - 1)^2$ (32)

• CT Zone :

By substituting equation (15) - which defines the allocation of the minimum core thickness in the upper floors of the tower - into equation (14), we obtain:

$$\ddot{\ddot{\Delta}}(z) - \Omega_e^4 \cdot \Delta(z) = 0 \tag{33}$$

Where a new variable is defined,
$$\Omega_e^4 = \frac{\Omega^2}{e_{min}}$$
 (34)

And this, considering that four overdots indicate the fourth derivative of Δ with respect to

$$z: \ddot{\Delta}(z) = \frac{\partial^4}{\partial z^4} \, \Delta(z) \tag{35}$$

The solution to this fourth-order differential equation is obtained by constructing its characteristic equation, based on the assumption of the following solution candidate function: $\Delta(z) = A \cdot e^{pz}$, where: $A \in \mathbb{R}$ and $p \in \mathbb{C}$. (36)

The characteristic equation is as follows:
$$A.e^{pz}.(p^4 - \Omega_e^4) = 0$$
 (37)

This leads us to two potential solutions:
$$p = \pm \Omega_e$$
 or, $p = \pm \Omega_e$. i (38)

Where, $i \in \mathbb{C}$ and it's the symbol of the imaginary unit. Therefore:

$$\Delta_{CT}(z) = \alpha_1 \cdot e^{\Omega_e \cdot z} + \alpha_2 \cdot e^{-\Omega_e \cdot z} + \alpha_3 \cdot \sin(\Omega_e \cdot z) + \alpha_4 \cos(\Omega_e \cdot z)$$
 (39)

By introducing a change of variable, we deduce that:

$$\Delta_{CT}(\bar{z}) = \alpha_1 \cdot e^{\bar{\Omega}_{e}.\bar{z}} + \alpha_2 \cdot e^{-\bar{\Omega}_{e}.\bar{z}} + \alpha_3 \cdot \sin(\bar{\Omega}_{e}.\bar{z}) + \alpha_4 \cos(\bar{\Omega}_{e}.\bar{z}) \tag{40}$$

Where in according to (34),
$$\bar{\Omega}_e^4 = (\Omega_e, H)^4 = \frac{\Omega^2}{e_{min}} \cdot H^4$$
 (41)

And the coefficients α_1 , α_2 , α_3 and $\alpha_4 \in \mathbb{R}$.

All belonging will be determined based on the boundary, displacement continuity, and slope continuity conditions (Conditions 2, 3, 6, and 7) specified in equations (4), (5), (19), and (20).

By applying equations (4) and (5), we obtain:
$$\begin{cases} \alpha_3 = \alpha_1 - \alpha_2 \\ \alpha_4 = \alpha_1 + \alpha_2 \end{cases}$$
 (42)

In turn, the equations (19) and (20) yield the following simplified results considering (40), (41), (42), (31), and (32):

$$\forall \, \bar{z} \in [0; \bar{z}_{cr}] : \Delta_{CT}(\bar{z}) = \psi_{\nu}.\bar{\Delta}_{CT}(\bar{z}) \tag{43}$$

Where: ψ_{ν} is defined in equation (32),

$$\bar{\Delta}_{CT}(\bar{z}) = \left[\bar{\alpha}_{1}.T_{1}(\bar{z})_{|\bar{\Omega}_{e}|} + \bar{\alpha}_{2}.T_{2}(\bar{z})_{|\bar{\Omega}_{e}|}\right]$$

$$\text{And}: \begin{cases}
\bar{\alpha}_{1} = {\alpha_{1} \choose \psi_{\nu}} = \left[\bar{T}_{4}.\bar{z}_{cr}^{2} + 2.\left(\frac{\bar{T}_{2}}{\bar{\Omega}_{e}} - \bar{T}_{4}\right).\bar{z}_{cr} - \left(\frac{2\bar{T}_{2}}{\bar{\Omega}_{e}} - \bar{T}_{4}\right)\right]/(2.\bar{T}_{5})$$

$$\bar{\alpha}_{2} = {\alpha_{2} / \psi_{\nu}} = \left[\bar{T}_{3}.\bar{z}_{cr}^{2} - 2.\left(\frac{\bar{T}_{6}}{\bar{\Omega}_{e}} + \bar{T}_{7}\right).\bar{z}_{cr} + \left(\frac{2\bar{T}_{1}}{\bar{\Omega}_{e}} + \bar{T}_{3}\right)\right]/(2.\bar{T}_{5})$$

With: $\bar{\eta} = \bar{\Omega}_e$. \bar{z}_{cr} and $\bar{\Omega}_e$ is defined in equation (41),

$$\begin{cases} \bar{T}_1 = T_1(\bar{z}_{cr})_{|\bar{\Omega}_e|} = e^{\bar{\Omega}_e.\bar{z}_{cr}} + \sin(\bar{\Omega}_e.\bar{z}_{cr}) + \cos(\bar{\Omega}_e.\bar{z}_{cr}) = e^{\bar{\eta}} + \sin(\bar{\eta}) + \cos(\bar{\eta}) \\ \bar{T}_2 = T_2(\bar{z}_{cr})_{|\bar{\Omega}_e|} = e^{-\bar{\Omega}_e.\bar{z}_{cr}} - \sin(\bar{\Omega}_e.\bar{z}_{cr}) + \cos(\bar{\Omega}_e.\bar{z}_{cr}) = e^{-\bar{\eta}} - \sin(\bar{\eta}) + \cos(\bar{\eta}) \\ \begin{cases} \bar{T}_3 = T_3(\bar{z}_{cr})_{|\bar{\Omega}_e|} = e^{\bar{\Omega}_e.\bar{z}_{cr}} - \sin(\bar{\Omega}_e.\bar{z}_{cr}) + \cos(\bar{\Omega}_e.\bar{z}_{cr}) = e^{\bar{\eta}} - \sin(\bar{\eta}) + \cos(\bar{\eta}) \\ \bar{T}_4 = T_4(\bar{z}_{cr})_{|\bar{\Omega}_e|} = e^{-\bar{\Omega}_e.\bar{z}_{cr}} + \sin(\bar{\Omega}_e.\bar{z}_{cr}) + \cos(\bar{\Omega}_e.\bar{z}_{cr}) = e^{-\bar{\eta}} + \sin(\bar{\eta}) + \cos(\bar{\eta}) \\ \bar{T}_5 = T_5(\bar{z}_{cr})_{|\bar{\Omega}_e|} = \left[\left(e^{\bar{\Omega}_e.\bar{z}_{cr}} + e^{-\bar{\Omega}_e.\bar{z}_{cr}} \right) .\cos(\bar{\Omega}_e.\bar{z}_{cr}) + 2 \right] = \left[\left(e^{\bar{\eta}} + e^{-\bar{\eta}} \right) .\cos(\bar{\eta}) + 2 \right] \\ \begin{cases} \bar{T}_6 = T_6(\bar{z}_{cr})_{|\bar{\Omega}_e|} = e^{\bar{\Omega}_e.\bar{z}_{cr}} - \sin(\bar{\Omega}_e.\bar{z}_{cr}) - \cos(\bar{\Omega}_e.\bar{z}_{cr}) = e^{\bar{\eta}} - \sin(\bar{\eta}) - \cos(\bar{\eta}) \\ \bar{T}_7 = T_7(\bar{z}_{cr})_{|\bar{\Omega}_e|} = e^{\bar{\Omega}_e.\bar{z}_{cr}} + \sin(\bar{\Omega}_e.\bar{z}_{cr}) - \cos(\bar{\Omega}_e.\bar{z}_{cr}) = e^{\bar{\eta}} + \sin(\bar{\eta}) - \cos(\bar{\eta}) \end{cases}$$

Key Step 4: The thickness function

The thickness function e(z) (or $e(\overline{z})$) represents an optimal vertical distribution of the tower's central core bracing aimed to upgrade and improve its seismic response. This function is defined separately over the two structural regions as follows:

VT Zone:

By making the substitution of equations (28) into equation (14), the following expression is obtained:

$$\ddot{e}(z) = \frac{\Omega^2}{\nu} \cdot \Delta(z) \tag{45}$$

So,
$$\ddot{e}(\bar{z}) = \frac{d^2 e(\bar{z})}{d\bar{z}^2} = H^2 \cdot \frac{d^2 e(\bar{z})}{d\bar{z}^2} = \frac{\Omega^2 \cdot H^2}{\nu} \cdot \Delta(\bar{z})$$
 (46)

Therefore, considering the scope of the two defined zones and through a double integration process of equation (46), we obtain:

$$e(\bar{z}) = \frac{\Omega^{2} \cdot H^{2}}{\nu} \cdot \left[\int_{0}^{\bar{z}} \int_{0}^{\bar{z}_{cr}} \Delta_{CT}(\bar{z}) \cdot d^{2}\bar{z} + \int_{0}^{\bar{z}} \int_{\bar{z}_{cr}}^{\bar{z}} \Delta_{VT}(\bar{z}) \cdot d^{2}\bar{z} \right]$$
(47)

By using equations (31), (32), (41), and (43), equation (47) will be:

$$e(\bar{z}) = \frac{1}{2} \bar{\Omega}_{e}^{4}. e_{min}. \left[\int_{0}^{\bar{z}} \int_{0}^{\bar{z}_{cr}} \bar{\Delta}_{CT}(\bar{z}). d^{2}\bar{z} + \int_{0}^{\bar{z}} \int_{\bar{z}_{cr}}^{\bar{z}} \bar{\Delta}_{VT}(\bar{z}). d^{2}\bar{z} \right]$$
(48)

Based on equations (32) and (44), and after calculating the double integration appearing in equation (48), the thickness function will be expressed as:

$$\forall \bar{z} \in [\bar{z}_{cr}; 1]: e(\bar{z}) = e_{VT}(\bar{z}) = \frac{1}{24} \bar{\Omega}_e^4 \cdot e_{min} \cdot [\bar{z}^4 - 4.\bar{z}^3 + 6.\bar{z}^2 + 12(\bar{T}_0 - \bar{k}_{cr}).\bar{z}]$$

$$e(\bar{z}) = e_{VT}(\bar{z}) = \frac{1}{24} \bar{\Omega}_e^4 \cdot e_{min} \cdot [\bar{z}^4 - 4.\bar{z}^3 + 6.\bar{z}^2 + 12(\bar{T}_0 - \bar{k}_{cr}).\bar{z}]$$
(49)

Where, $\bar{\Omega}_e$ is defined in equation (41),

$$\bar{k}_{cr} = k(\bar{z}_{cr}) = \frac{\bar{z}_{cr}^3}{3} - \bar{z}_{cr}^2 + \bar{z}_{cr}$$
 (50)

And, $\overline{T}_0 = \frac{1}{\overline{\Omega}_e} \cdot (\overline{\alpha}_1 \cdot \overline{T}_7 - \overline{\alpha}_2 \cdot \overline{T}_8)$; knowing that these components have been defined in equation (44).

• CT Zone:

From the above, we save the following formula (15):

$$\forall \bar{z} \in [0, \bar{z}_{cr}] : e(\bar{z}) = e_{cT}(\bar{z}) = e_{min}$$

Key Step 5 – Final: Relationship between the unknowns \bar{z}_{cr} and $\bar{\Omega}_e$

To establish the sought-after relationship between the two unknowns, we introduce two additional conditions, referred to as Condition 8 and Condition 9. They respectively express the continuity of the thickness function, and the limitation of material usage, while maintaining a mastered average thickness, denoted e_m .

The conditions are defined as follows:

• Thickness function continuity condition:

Condition 8:
$$e_{CT}(\bar{z}_{cr}) = e_{VT}(\bar{z}_{cr})$$
 (51)

• Optimal mastery of the construction material usage condition:

Condition 9: As mentioned in equation (18):
$$\int_0^1 e(\bar{z})d\bar{z} = e_m$$
 (52)

These two conditions in equations (51) and (52) can be reformulated into alternative expressions, derived also from equation (15):

$$e_{VT}(\bar{z}_{cr}) = e_{min} \tag{53}$$

And,
$$\int_{\bar{z}_{cr}}^{1} e_{VT}(\bar{z}) d\bar{z} = e_m - e_{min}.\bar{z}_{cr}$$
 (54)

By substituting equations (49) and (50) into equation (53), we obtain the first relationship between the unknowns \overline{z}_{cr} and $\overline{\Omega}_{e}$:

$$\bar{z}_{cr}^{4} - \frac{8}{3}.\bar{z}_{cr}^{3} + 2.\bar{z}_{cr}^{2} = 4.\left[\bar{T}_{0}.\bar{z}_{cr} - \frac{2}{\bar{\Omega}_{e}^{4}}\right]$$
 (55)

And the second one is deduced by substituting equations (49) and (50) into equation (54):

$$k_{\rm m} = \left\{ \frac{1}{120} \cdot \overline{\Omega}_{\rm e}^{4} \cdot \left[9 \cdot \overline{z}_{\rm cr}^{5} - 25 \cdot \overline{z}_{\rm cr}^{4} + 10 \cdot \overline{z}_{\rm cr}^{3} + 30(1 - \overline{T}_{0}) \cdot \overline{z}_{\rm cr}^{2} + 30 \left(\frac{4}{\overline{\Omega}_{\rm e}^{4}} - 1 \right) \cdot \overline{z}_{\rm cr} + 30 \cdot \overline{T}_{0} + 6 \right] \right\}$$
(56)

Where,
$$k_m = \frac{e_m}{e_{min}}$$
 (57)

Table 1: Values of \overline{z}_{cr} , $\overline{\Omega}_{e}$ and \overline{T}_{0} for each input value of \mathcal{R}_{m}

k_m	73,956	17,523	7,683	4,440	3,019	2,285	1,861	1,596	1,421	1,299
\bar{z}_{cr}	0,05	0,10	0,15	0,20	0,25	0,30	0,35	0,40	0,45	0,50
$\overline{\Omega}_{ m e}$	6,175	4,247	3,369	2,836	2,467	2,193	1,979	1,806	1,663	1,542
\overline{T}_0	0,051	0,105	0,164	0,230	0,303	0,385	0,477	0,580	0,694	0,822
k_m	1,213	1,150	1,104	1,070	1,045	1,026	1,014	1,006	1,001	1,000
\bar{z}_{cr}	0,55	0,60	0,65	0,70	0,75	0,80	0,85	0,90	0,95	1,00
$\overline{\Omega}_{ m e}$	1,439	1,349	1,270	1,201	1,139	1,083	1,032	0,987	0,945	0,907
\overline{T}_0	0,964	1,121	1,294	1,484	1,692	1,920	2,168	2,437	2,728	3,042

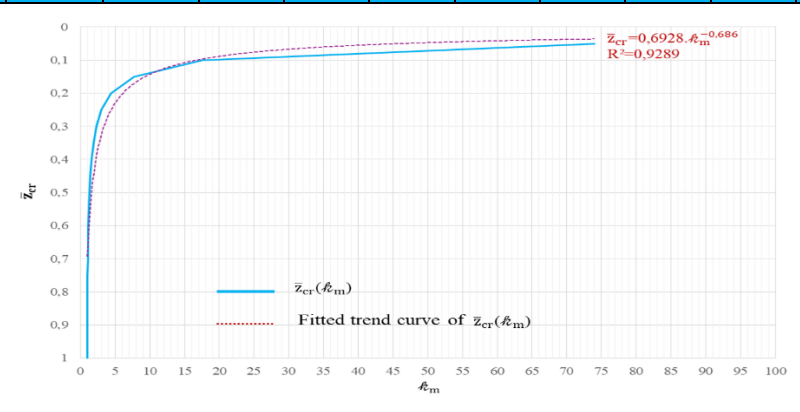


Fig. 3. Graph illustrating the relationship between \bar{z}_{cr} and k_m .

By developing a simple algorithm in Python code, the values of \overline{z}_{cr} corresponding to $\overline{\Omega}_{e}$ can be obtained from equation (55), by progressively varying \overline{z}_{cr} in increments of 0.05 within the interval between 0 and 1 ($\overline{z}_{cr} \in [0;1]$). This relationship between \overline{z}_{cr} and $\overline{\Omega}_{e}$ appears to be of significant value for establishing their numerical correlation with the coefficient k_m , through the application of equation (56). This enabled the construction of a ready-to-use table, as shown in Table 1, displaying, for each input

value of k_m , the associated values of \bar{z}_{cr} , $\bar{\Omega}_e$ and \bar{T}_0 , and facilitated the direct representation of the graph in Figure 3, illustrating the relationship between \bar{z}_{cr} and k_m .

V. Practical Guideline for the Structural Design Engineer

This practical guideline is structured around three milestones, each easy to assimilate and simple to implement. They are presented as follows:

First milestone

To implement this targeted methodological procedure, the Structural Engineer will also draw upon their professional expertise. The input parameters to be defined include:

- The tower height, denoted H, as specified in the architectural drawings,
- The minimum thickness of the central core bracing of the tower, denoted e_{min}, which should be derived from seismic regulations and best practices in Civil Engineering,
- The average thickness of the central core bracing of the tower, denoted e_m, considered as *an iterative value* framing the optimization of material quantities and associated costs.

Result 1: the value of the dimensionless coefficient k_m is derived from equation (57).

Second milestone

Then, using this calculated value of k_m , the critical relative height \bar{z}_{cr} can be determined directly from the Table 1 or Figure 3.

Result 2: the value of the critical relative height \overline{z}_{cr} is now known.

Third milestone

Based on the preceding calculations, the optimal variation of thickness $e(\overline{z})$, as proposed in the present article, can be determined by applying equations (49) and (15), which govern the thickness distribution of the central core bracing of the tower across the CT zone and VT zone (constant thickness zone and variable thickness zone).

Result 3: the thickness functions $e_{VT}(\bar{z})$ and $e_{CT}(\bar{z})$ are now known. The targeted design is thus defined, and the engineering analysis process can follow.

VI. Case study – Illustrative application

Brief Introduction

The case study examines a representative R+32 tower with four basement levels (H=121 m), planned as part of a major urban development project for a new Financial City in Morocco [XI].

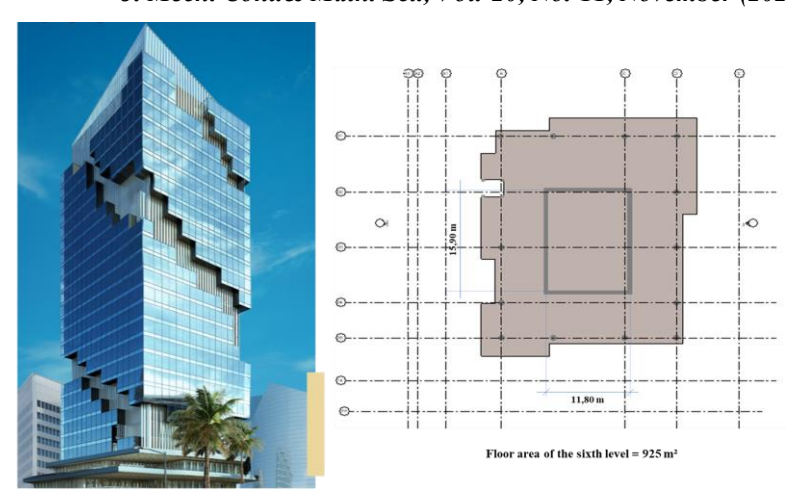


Fig. 4. Elevation view of the studied tower and section of the central bracing core for a typical floor plan

Figure 4 displays the elevation view of the tower along with the key dimensions of the central bracing core in a typical plan layout. Dynamic modal analysis is carried out using specialized software (RSA 2025), dedicated to educational and research purposes. The analysis is based on the thickness distribution framework proposed in the present paper.

Contextualization and studied variants

Two design variants are considered within this illustrative application in the aim of illustrating the potential efficiency gains achievable through our proposed pre-sizing methodology:

- The first variant (adopted by the engineering design office and architectural configuration reference case) assumes a constant central core thickness, set at e = 50 cm = constant value. This thickness is considered the reference thickness for the comparison study.
- The second variant faithfully follows the proposed practical guideline, incorporating a significantly reduced quantity of material, represented by an average thickness of $e_m = 40$ cm. The thickness distribution reaches its termination at the top of the tower, with a minimum value of $e_{min} = 22$ cm, leading, therefore, to a coefficient value of $k_m = 1,818$, using equation (57) and the first milestone requirements.

For this second variant, the numerical application, based on the implementation of the second aforementioned milestone, yields the following results, as shown in Table 2.

Table 2: Value of \bar{z}_{cr} and z_{cr} according to the input value of k_m (Variant 2)

e _m (cm)	e _{min} (cm)	₿ _m	$\bar{\mathbf{z}}_{cr}$	$\mathbf{z}_{cr} = \overline{\mathbf{z}}_{cr}.H(m)$
40	22	1,818	0,358	43,33

For practical and scheduling reasons related to the construction process, particularly to facilitate the implementation of slipform systems for casting the shear walls forming the tower's central bracing core, we opted to apply vertical thickness variation by subdividing the tower's height into four sections, ranging from the minimum thickness at the top to the maximum at the base:

- The first section at the top of the tower spans from 0 m to 65 m, encompassing 18 levels (from floor 15 to floor 32),
- The second section in the mid-zone extends from 65 m to 86 m, comprising 6 levels (from floor 9 to floor 14),
- The third section, also mid-zone, ranges from 86 m to 110 m, covering 7 levels (from floor 2 to floor 8),
- The fourth section at the base of the tower spans from 110 m to 121 m, comprising 2 major levels (the ground floor and first floor). The four basement levels are assigned the same thickness as the ground floor.

So, based on the implementation of the third aforementioned milestone, the numerical application leads to the thickness distribution of the central core bracing of the tower, deemed to be the optimal solution, as shown in Figure 5, where :

•
$$e_1 = e_{CT} (0 \le \bar{z} \le 0.537) = e_{min} = 22 \ cm$$

•
$$e_2 = e_{VT}(0.537 \le \bar{z} \le 0.713) = e_{VT}(0.537) = 37 \text{ cm}$$

•
$$e_3 = e_{VT}(0.713 \le \bar{z} \le 0.907) = e_{VT}(0.713) = 54 \text{ cm}$$

•
$$e_4 = e_{VT}(0.907 \le \bar{z} \le 1.000) = e_{VT}(0.907) = 70 \text{ cm}$$
 (58)

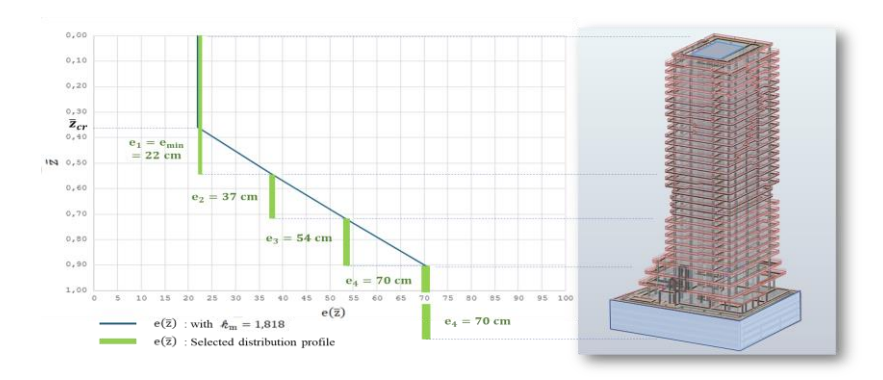


Fig. 5: Plot of the thickness distribution of the central core bracing of the tower and software modeling (Variant 2)

Comparative Analysis

The two studied design variants exhibit distinct behaviors in terms of displacements, modal participation, and dynamic characteristics, as shown in Table 3.

Table 3: Modal analysis findings and seismic displacement check (Variant 2)

Dynamic mode number	Frequency (Hz)	Frequency in the first dynamic mode (Hz)	Cumulative mobilized masses in the X-direction (%)	Cumulative mobilized masses in the Y-direction (%)	Maximum global displacement at the top of the tower (mm)			
	Variant 1: Constant Thickness							
50	3,55	0,17	70,45	71,39	53,90			
	Variant 2: Variable Thickness							
41	13,46	0,22	90,95	90,12	42,40			
	Benefits assessment of the Variant 2							
✓	+↑ 279,15 %	+↑ 29,41 %	√	→	- \ 21,33 %			

Variant 1, representing the initial design, shows a high overall absolute displacement exceeding the normative and regulatory admissible threshold. Indeed, its peak value reaches approximately 54 mm at the top of the tower. It also displays insufficient modal mass participation (around 70%), despite mobilizing more than 50 dynamic deformation modes. This observation indicates that the structure in Variant 1 is highly rigid, concentrating seismic energy and further internalizing dynamic strengths. This conclusion is supported by the low natural frequency value in the first mode of modal analysis (0.17 Hz), as well as the slow frequency progression up to mode 50 (reaching 3.55 Hz).

Variant 2, on the other hand, reflects a validated seismic design, achieving mass mobilization exceeding 90% in both lateral directions in mode 41. These modal mass values demonstrate the structural resistance through seismic energy dissipation via finely mastered deflections. Furthermore, Variant 2 confirms that varying the thickness of central core bracing, following the method proposed in the present paper, significantly improves and upgrades the tower's dynamic seismic performance. This includes maximizing the first modal frequency (0.22 Hz), reflecting an increase of over 29%, and a rapid frequency progression up to mode 41 (13.46 Hz), while maintaining a well-controlled overall deformation (around 42 mm at the top of the tower—a reduction of more than 21%).

This analysis relies on optimizing the quantity of concrete used in the central core. Based on the adjusted thicknesses shown in Figure 5, Variant 2 demonstrates a substantial volume reduction of over one-third. This structural optimization methodology strongly supports the efficient allocation of investments in these slender structures.

V. Conclusion

Accordingly, this study relies on the free vibration equation of a cantilever beam (fixed at its base and free at its top) [XVI], and incorporates mechanically intuitive parameters easily grasped by practicing civil engineers, such as wall thickness, inertia, natural frequency, fundamental pulsation, and general/inter-story displacement. This easy-to-use parametric study fully aligns with the goals of financial optimization, resource rationalization, and effective upgrading of both modal dynamic response and seismic performance, through the targeted adjustment of the fundamental frequency of the modeled structural system.

This study is seamlessly integrated into the framework of preliminary structural design for slender towers braced by a central core, particularly concerning mastering their projected dynamic and seismic behavior.

To this end, a practical guideline dedicated to civil design engineers and relating to slender structures was developed. It aimed at reducing the quantity of construction material required and optimizing the system's natural frequency, specifically, by maximizing its smallest eigenvalue. The analytical—parametric investigation proposes solving this max—min formulation, subject to material optimization constraints, through detailed derivations of the core thickness profile across two structural zones. Accordingly, a critical relative height was defined to demarcate the threshold between the zone of constant minimum thickness and the zone with variable thickness.

This methodological approach directs the dynamic structural response toward a more mature and targeted optimal design, thereby upgrading dynamic characteristics identified via modal analysis, while significantly reducing both the iterative computational time and the cost of material consumption. It is based on mechanically intuitive parameters easily grasped by practicing civil engineers.

This research paper culminates in a concrete case study applying the proposed methodology and exhibiting the expected positive impacts.

Conflict of Interest:

There was no relevant conflict of interest regarding this paper.

References

- I. Abdi F.,: 'Understanding the impact of high-rise buildings on environmental quality and sustainable urban development'. *Journal of Art and Architecture Studies*. Vol. 8(2), pp. 13-18, 2019. 10.51148/jaas.2019.3
- II. Al Agha W., Almorad W. A., Umamaheswari N., Alhelwani A.,: 'Study the seismic response of reinforced concrete high-rise building with dual framed-shear wall system considering the effect of soil structure interaction'. *Materials today proceedings*. Vol. 43(2), pp. 2182-2188, 2021. 10.1016/j.matpr.2020.12.111.

- III. Alavi A., Rahgozar P., Rahgozar R.,: 'Minimum-Weight Design of High-Rise Structures Subjected to Flexural Vibration at a Desired Natural Frequency'. *Structural Design of Tall and Special Buildings*. Vol. 27(15), pp. 1-13, 2018. 10.1002/tal.1515.
- IV. Bao L., Yicong F., Graeme J. K.,: 'Topology optimization using an eigenvector aggregate'. *Structural and Multidisciplinary Optimization*. Vol. 66(221), pp. 1–19, 2023. 10.1007/s00158-023-03674-x.
- V. Davari S. M., Malekinejad M., Rahgozar R.,: 'An approximate approach for the natural frequencies of tall buildings with trussed-tube system'. *Innovative Infrastructure Solutions*. Vol. 6(46), pp. 1-9, 2021. 10.1007/s41062-020-00418-4.
- VI. Davidovici V., : 'La construction en zone sismique'. Le Moniteur. 1999.
- VII. Dym Clive L. P. E., Williams Harry E.,: 'Estimating Fundamental Frequencies of Tall Buildings'. *Journal of Structural Engineering*. Vol. 133(10), pp. 1-5, 2007.
- VIII. Haopeng L., Zhibin X., Yinyuan W., Guan Q., Fengling J., Boqing G., Hongjia L.,: 'Size optimization design of members for shear wall high-rise buildings'. *Journal of Building Engineering*. Vol. 61 (105292), pp. 27–37, 2022. 10.1016/j.jobe.2022.105292.
- IX. Keihani R., Bahadori-Jahromi A., Goodchild C., Cashell K. A.,: 'The influence of different factors on buildings'. *Structural Engineering and Mechanics*. Vol. 76(1), pp. 83-99, 2020. 10.12989/sem.2020.76.1.083.
- X. Lam T. Q. K., Ho C. C.,: 'Shear wall thickness affects high-rise building internal force and horizontal displacement according to TCVN 2737:2023'. *Journal of Materials & Construction*. Vol. 14 (2), pp. 27–37, 2024. 10.54772/jomc.v14i02.798.
- XI. M-Tower Project website, mtower.ma/
- XII. Nieto F., Montoya M.C., Hernandez S.,: 'Shape Optimization of Tall Buildings Cross-Section: Balancing Profit and Aeroelastic Performance'. *The Structural Design of Tall and Special Buildings*. Vol. 31(18), pp. 1-21, 2022. 10.1002/tal.1982.
- XIII. Nitti G., Lacidogna G., Carpinteri A.,: 'An analytical formulation to evaluate natural frequencies and mode shapes of high-rise buildings'. *Curved and Layered Structures*. Vol. 8, pp. 307-318, 2021. 10.1515/cls-2021-0025.
- XIV. Patel T., Singh P., Dhaakad D., Vaghela S., Chauhan R., Maseleno A., Isnanto R. R.,: 'Optimization techniques in real estate investment portfolios: A quantitative approach'. *Greenation International Journal of Engineering Science*. Vol. 1(4), pp. 183-194, 2024. 10.38035/gijes.v1i4

- XV. Patil R., Deshpande A.S., Sambanni S.,: 'Optimal location of shear wall in high rise building subjected to seismic loading'. *International Journal For Technological Research In Engineering*. Vol. 3(10), pp. 2347-4718, 2016.
- XVI. Paz M., Leigh W.,: Structural Dynamics: 'Theory and Computation; Updated with SAP 2000'. 5th Edition, Kluwer Academic Publishers, USA, 2004.
- XVII. Rahzogar P.,: 'Free Vibration of Tall Buildings using Energy Method and Hamilton's Principle'. *Civil Engineering Journal*. Vol. 6(5), pp. 945–953, 2020. 10.28991/cej-2020-03091519.
- XVIII. Rahgozar R., Safari H., Kaviani P.,: 'Free vibration of tall buildings using Timoshenko beams with variable cross-section'. WIT Transactions on the Built Environment, Structures Under Shock and Impact VIII. Vol. 73(15), pp. 233-242, 2004. 10.2495/SU040231.
- XIX. Robot Structural Analysis Professionnal (RSA 2025) website, www.autodesk.com/products/robot-structural-analysis/overview
- XX. Rossmann J. S., Dym Clive L. P. E., Bassman L.,: 'Introduction to Engineering Mechanics: A Continuum Approach'. CRC Press, 2nd Edition, Boca Raton, USA, 2015.
- XXI. Tao L., Bin L., Shuting W., Liang G.,: 'Eigenvalue topology optimization of structures using a parameterized level set method'. *Structural and Multidisciplinary Optimization*. Vol. 50, pp. 573–591, 2014. 10.1007/s00158-014-1069-z.
- XXII. Yaghoobi N., Hassani B.,: 'Topological optimization of vibrating continuum structures for optimal natural eigenfrequency'. *International journal of optimization in civil engineering*. Vol. 7(1), pp. 1-12, 2017.